DALTON

Characteristics of acid-catalysed substitution mechanisms and sites of protonation in iron–sulfur-based clusters, as revealed by studies on $[Cl_2FeS_2VS_2FeCl_2]^{3-}$*

Karin L. C. Grönberg and Richard A. Henderson

John Innes Centre, Nitrogen Fixation Laboratory, Norwich Research Park, Colney, Norwich NR4 7UH, UK

The kinetics of the non-catalysed and acid-catalysed substitution of the first two chloride ligands of $[Cl_2FeS_2VS_2FeCl_2]^{3-}$, by 4-$RC_6H_4S^-$ to form $[(4\text{-}RC_6H_4S)ClFeS_2VS_2FeCl(SC_6H_4R\text{-}4)]^{3-}$ (R = Cl, H, Me or MeO), has been studied in MeCN at 25.0 °C using stopped-flow spectrophotometry. Whereas the non-catalysed substitution occurs by a dissociative mechanism, the acid-catalysed substitution (using $[NHEt_3]^+$ as the acid) is associative. In the acid-catalysed mechanism the rate of substitution is maximised when protonation and binding of the nucleophile occur at adjacent sites. Two features of this study appear to be general for a range of structurally different iron–sulfur-based clusters: (1) the proton affinities of the clusters and (2) the acid-catalysed substitution mechanisms. These aspects are discussed for a variety of iron–sulfur-based clusters, including $[(MoFe_3S_4Cl_3)_2\{\mu\text{-}Fe(SEt)_6\}]^{3-}$.

Iron–sulfur-based clusters are the substrate binding sites of metalloenzymes such as nitrogenases, hydrogenases and aconitase.[1] Despite this, little is understood about how this type of cluster binds small molecules or undergoes substitution reactions. A general protocol for defining the kinetics of the substitution and acid-catalysed substitution reactions has been established, using the system outlined in Scheme 1.[2] By supplying the thiolate nucleophile as the tetraalkylammonium salt, and controlling the relative proportions of $[NHEt_3]^+$ and thiolate ion, the influence that acid, base and nucleophile concentrations have on the rate of the reaction can be established unambiguously. In this manner the reaction mechanisms of structurally well-defined, synthetic iron–sulfur-based clusters are being developed, particularly defining: (*i*) the influence of acid on the lability of the cluster; (*ii*) the intimate mechanisms of substitution and (*iii*) the way in which individual components contribute to the reactivity of the cluster as a whole.

In this paper the kinetics of substitution reactions of $[Cl_2FeS_2VS_2FeCl_2]^{3-}$ with 4-$RC_6H_4S^-$ (R = Cl, H, Me or MeO), both in the presence and absence of acid, is described. This work indicates, for the first time, that the associative mechanism of acid-catalysed reactions requires the proton to be bound adjacent to the site of substitution, and discusses: (1) general proton affinities of a variety of iron–sulfur-based clusters and (2) how this stereochemical relationship between the sites of substitution and protonation can be applied to these clusters.

Experimental

All manipulations were performed under an atmosphere of dinitrogen or argon using standard Schlenk or syringe techniques. The clusters used, $[NEt_4]_3[Cl_2FeS_2VS_2FeCl_2]$[3] [Found (Calc.): C, 50.8 (51.6); H, 7.1 (7.2); N, 3.4 (3.8)%] and $[NEt_4]_3[Mo_2Fe_7S_8(SEt)_6Cl_6]$[4] [^{1}H NMR spectrum: δ 39.0, 27.1 (μ-SCH_2); −1.6 (μ-SCH_2CH_3)], were prepared and recrystallised according to the literature. Products were confirmed by elemental analysis, UV/VIS and/or ^{1}H NMR spectroscopy. The ^{1}H NMR spectra were recorded on a JEOL GSX 270 spectrometer using CD_3CN as solvent and $SiMe_4$ as reference.

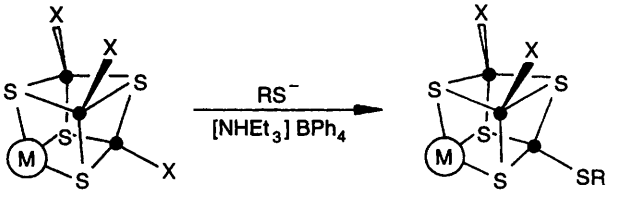

Scheme 1 General system for studying the kinetics of substitution of iron–sulfur-based clusters

Mössbauer spectra were recorded on a ES-Technology MS105 spectrometer. Parameters were determined at 77 K by using a 925 MBq ^{57}Co source in a rhodium matrix, and were referenced against iron foil at 298 K. The samples were prepared by using a 40 mmol dm^{-3} solution of $[Cl_2FeS_2VS_2FeCl_2]^{3-}$, to which the calculated amount of $[NEt_4][SPh]$ was added. The reaction solution was transferred by gas-tight syringe to the sample holder and immediately frozen in liquid nitrogen. Spectra were recorded for *ca.* 72 h.

The salt $[NEt_4]Cl$ was dried (80 °C, *in vacuo*) prior to use and $[NEt_4][SC_6H_4R\text{-}4]$ (R = H, Me, MeO or Cl)[4] and $[NHEt_3][BPh_4]$[5] were prepared by the literature methods and recrystallised from acetonitrile–diethyl ether. Acetonitrile used in the kinetic studies was freshly distilled from CaH_2 immediately prior to use. Solutions for the stopped-flow studies were prepared and used within 1 h.

Kinetic experiments

All solutions were prepared under an atmosphere of dinitrogen and transferred by gas-tight glass syringe to the Hi-Tech Scientific SF-51 stopped-flow spectrophotometer, modified to handle air-sensitive solutions.[6] The temperature was maintained at 25.0 °C by use of a Grant LE8 thermostat tank. The apparatus was interfaced to a Viglen 486 computer *via* an analogue-to-digital converter.

The reactions were studied (at λ = 500 nm for the $[Cl_2FeS_2VS_2FeCl_2]^{3-}$ cluster and in a range from λ = 450 to 700 nm for the $[Mo_2Fe_7S_8(SEt)_6Cl_6]^{3-}$ cluster) by monitoring

† *Supplementary data available* (No. SUP 57165, 10 pp.): first-order rate constants. See Instructions for Authors, *J. Chem. Soc., Dalton Trans.*, 1996, Issue 1. *Non-SI unit employed:* $\mu_B \approx 9.27 \times 10^{-24}$ J T^{-1}.

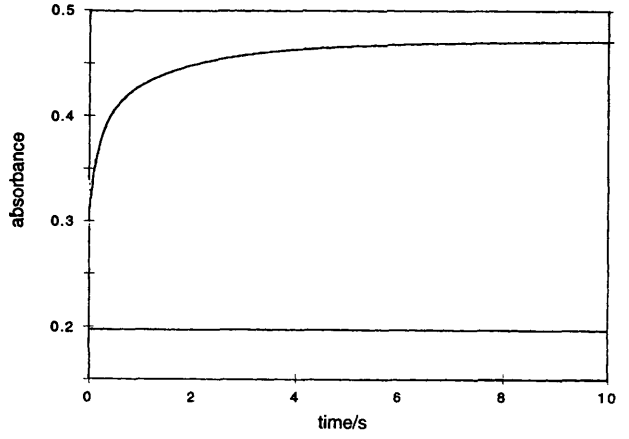

Fig. 1 Typical absorbance *vs.* time curve for the reaction of $[Cl_2FeS_2VS_2FeCl_2]^{3-}$ (0.05 mmol dm^{-3}) with PhS^- (50 mmol dm^{-3}), measured at λ = 500 nm in MeCN at 25.0 °C. The curve was fitted by two exponentials with rate constants $k_{obs}(1) = 5.0\ s^{-1}$ and $k_{obs}(2) = 0.56\ s^{-1}$, and the corresponding absorbance changes $\Delta A_1 = 0.096$ and $\Delta A_2 = 0.073$ respectively; $A_\infty = 0.471$. The absorbance of $[VFe_2S_4Cl_4]^{3-}$ is shown at $A = 0.198$

the absorbances of the clusters. These increase over time as the chloro-groups are substituted by thiolate. The exponential character of the observed curves was established by computer curve fitting.

When studied on a stopped-flow spectrophotometer, the reaction between $[Cl_2FeS_2VS_2FeCl_2]^{3-}$ and PhS^- is associated with an exponential absorbance *vs.* time trace in the initial phase as shown in Fig. 1. Similar traces were observed with the other thiolates.

Results and Discussion

Generally, in iron–sulfur-based clusters the iron sites are magnetically coupled or chemically distinct.[7] However, in the trinuclear, linear cluster $[Cl_2FeS_2VS_2FeCl_2]^{3-}$ the iron sites are chemirally equivalent, but the magnetic moment (7.01 μ_B)[3] indicates that they are magnetically isolated. Kinetic studies on the reactions of $[Cl_2FeS_2VS_2FeCl_2]^{3-}$ probe how these features influence the reactivity of this cluster. In particular, we have studied its substitution reactions with arenethiolate ions, both in presence and absence of acid, equation (1). Initially, the reaction in absence of acid will be discussed, and subsequently the acid-catalysed pathway will be described.

$$[Cl_2FeS_2VS_2FeCl_2]^{3-} + 2(4\text{-}RC_6H_4S^-) \xrightarrow{[NHEt_3]^+} [(RC_6H_4S)ClFeS_2VS_2FeCl(SC_6H_4R)]^{3-} + 2Cl^- \quad (1)$$

The uncatalysed reaction

A major problem in studying the reactions of chloro-substituted iron–sulfur-based clusters such as $[Cl_2FeS_2VS_2FeCl_2]^{3-}$ is the lack of spectroscopic handles associated with these complexes. There are no sufficiently diagnostic bands in the IR spectrum, nor peaks in the paramagnetically shifted NMR spectrum. Consequently, we have mostly used UV/VIS spectroscopy to follow reaction (1). However, the reaction was also monitored by using Mössbauer spectroscopy, as shown in Fig. 2. Mössbauer spectroscopy shows that, even at a ratio of 4:1 of PhS^- to $[Cl_2FeS_2VS_2FeCl_2]^{3-}$, both reactant and product are present. This indicates that the reaction is an equilibrium. Only at a ratio of 10:1 is there stoichiometric production of $[(PhS)_2FeS_2VS_2Fe(SPh)_2]^{3-}$. Consequently all kinetic studies were performed under conditions where $[4\text{-}RC_6H_4S^-]$: $[Cl_2FeS_2VS_2FeCl_2]^{3-} \geqslant 10:1$, where non-equilibrium conditions prevail.

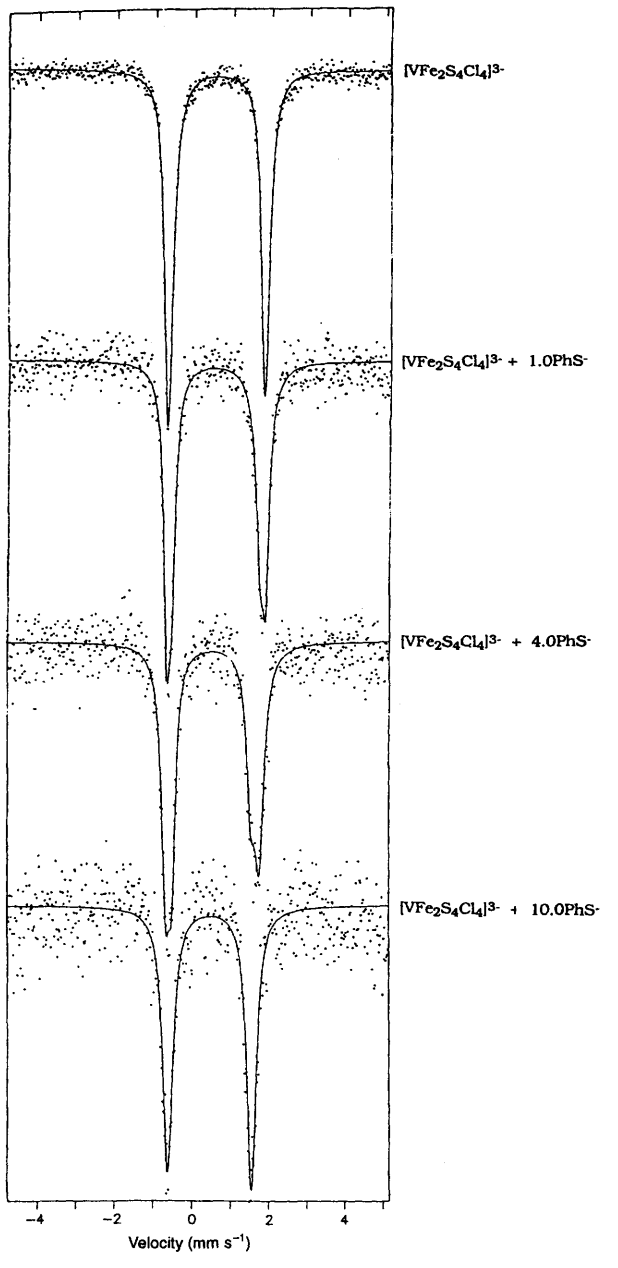

Fig. 2 Mössbauer spectra for the reaction of $[Cl_2FeS_2VS_2FeCl_2]^{3-}$ and PhS^- in MeCN. Top spectrum is that of $[Cl_2FeS_2VS_2FeCl_2]^{3-}$ (δ 0.620 ± 0.001 mm s^{-1}, Δ = 2.508 ± 0.002 mm s^{-1}), bottom spectrum is that of $[VFe_2S_4(SPh)_4]^{3-}$ (δ = 0.475 ± 0.005 mm s^{-1}, Δ = 2.165 ± 0.009 mm s^{-1})

When studied on a stopped-flow spectrophotometer, the reaction between $[Cl_2FeS_2VS_2FeCl_2]^{3-}$ and an excess of $4\text{-}RC_6H_4S^-$ exhibits the absorbance *vs.* time curve shown in Fig. 1. This trace corresponds to the substitution of all four chloro-groups in $[Cl_2FeS_2VS_2FeCl_2]^{3-}$ and can be adequately fitted by two exponentials of similar absorbance magnitude. The first of these exponentials corresponds to equation (1), and it is this reaction which will be discussed. The exponential nature of the absorbance *vs.* time curves, at all thiolate-ion concentrations, indicates that reaction (1) exhibits a first-order dependence on the concentration of the cluster. This is confirmed in experiments where the concentration of thiolate is kept constant, $[4\text{-}RC_6H_4S^-] = 5.0$ mmol dm^{-3}, whilst the

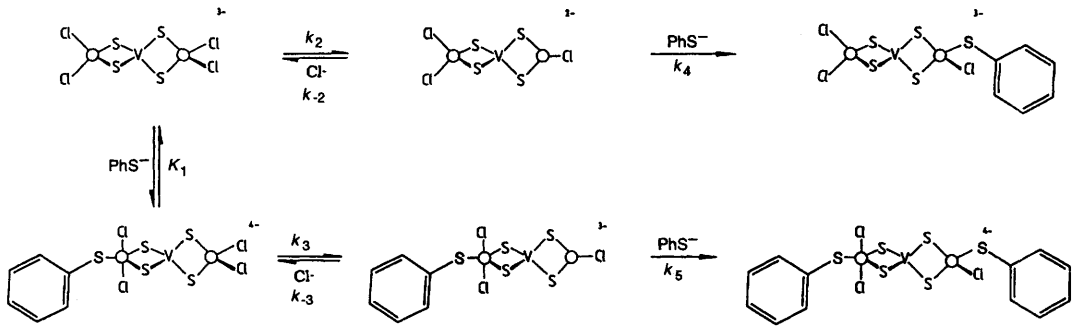

Scheme 2 Mechanism for the reaction of $[Cl_2FeS_2VS_2FeCl_2]^{3-}$ with thiolate

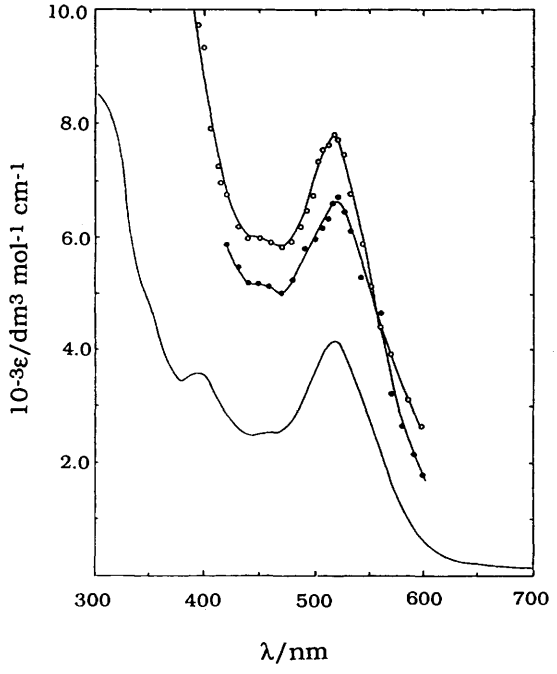

Fig. 3 The UV/VIS absorption spectra of $[Cl_2FeS_2VS_2FeCl_2]^{3-}$ (solid line) and the intermediate $[Cl_2FeS_2VS_2FeCl_2(SC_6H_4R\text{-}4)]^{4-}$ [R = H (●) or Cl (○)]

concentration of cluster is varied over the range $[Cl_2FeS_2VS_2FeCl_2{}^{3-}]$ = 0.013–0.2 mmol dm^{-3}. Under these conditions the observed first order rate constant does not vary, k_{obs} = 3.3 ± 1.0 s^{-1}. At all thiolate-ion concentrations the reaction is independent of both the concentration and the nature of 4-$RC_6H_4S^-$; k_{obs} = 3.3 ± 1.0 s^{-1} (R = Cl, H, Me or MeO).

The rate of substitution of the first two chloro-groups is insensitive to the concentration and nature of the thiolate ion, consistent with a dissociative mechanism as shown in Scheme 2. In this mechanism substitution can occur at either of the two chemically equivalent iron atoms by rate-limiting dissociation of a chloro-group to generate the cluster that contains a three-co-ordinate iron, $[Cl_2FeS_2VS_2FeCl]^{3-}$. Rapid attack of a thiolate ion at the vacant site completes the first substitution step. However, this is not the only reaction associated with the first exponential. Since the two iron sites in this trinuclear cluster are magnetically isolated they react independently. Thus, substitution of the second iron site occurs at a rate which is experimentally indistinguishable from that of the first. That the whole absorbance *vs.* time curve can be fitted by two exponentials with similar absorbance magnitudes is consistent with the proposal that the first exponential corresponds to the substitution of half of the chloro-groups in $[Cl_2FeS_2VS_2FeCl_2]^{3-}$.

The visible absorption spectrum of $[Cl_2FeS_2VS_2FeCl_2]^{3-}$ is shown in Fig. 3, and at low concentrations of thiolate the initial absorbance of the stopped-flow traces (λ = 500 nm) corresponds to this species. However, at high concentrations of thiolate ion the initial absorbance is markedly higher, as shown in Fig. 1. Indeed, this initial absorbance depends on the concentration of thiolate and quantitative analysis demonstrates that within 2 ms one thiolate binds in a rapid equilibrium to form $[Cl_2FeS_2VS_2FeCl_2(SC_6H_4R\text{-}4)]^{4-}$ (Table 1).

Table 1 Spectrophotometrically determined values of the binding constant (K_1) for the binding of 4-$RC_6H_4S^-$ (R = H, Me, MeO or Cl) to $[VFe_2S_4Cl_4]^{3-}$ in MeCN at 25.0 °C

R	[4-$RC_6H_4S^-$]/mmol dm^{-3}	Absorbance	K_1/dm^{3}mol^{-1}
H	1.25	0.211	105
	2.5	0.222	109
	5.0	0.235	98.5
	10.0	0.245	72.4
	20.0	0.261	64.2
	40.0	0.288	102.3
			Mean = 91.9
Cl	1.25	0.264	119.9
	2.5	0.275	163.3
	5.0	0.286	163.4
	10.0	0.291	109.2
	20.0	0.301	99.8
	40.0	0.313	131.8
			Mean = 131.2
Me	1.25	0.269	18.8
	2.5	0.281	29.6
	5.0	0.290	23.1
	10.0	0.311	22.5
	20.0	0.356	27.7
	40.0	0.454	68.3
			Mean = 31.7
MeO	1.25	0.308	60.0
	2.5	0.322	86.8
	5.0	0.377	305.4
	10.0	0.350	65.5
	20.0	0.372	65.2
	30.0	0.388	74.2
	40.0	0.408	136.3
			Mean = 113.3

The visible absorption spectra of $[Cl_2FeS_2VS_2FeCl_2(SC_6H_4R\text{-}4)]^{4-}$ (R = or Cl), measured on the stopped-flow apparatus at high concentrations of thiolate, are shown in Fig. 3. The spectra show well defined absorption peaks at 520 nm. The spectrum of the R = H species is more intense than that of R = Cl; this is a feature which parallels the relative intensities of the spectra of the corresponding final products. The peak maxima observed for $[Cl_2FeS_2VS_2FeCl_2(SC_6H_4R\text{-}4)]^{4-}$ are at the same wavelength as that of $[Cl_2FeS_2VS_2FeCl_2]^{3-}$. This is not unexpected since the spectra of both $[Cl_2FeS_2VS_2FeCl_2]^{3-}$ and $[Cl_2FeS_2VS_2FeCl_2(SC_6H_4R\text{-}4)]^{4-}$ are dominated by charge-transfer transitions from sulfur to vanadium. The major perturbation to the transitions of the VS_4 chromophore are

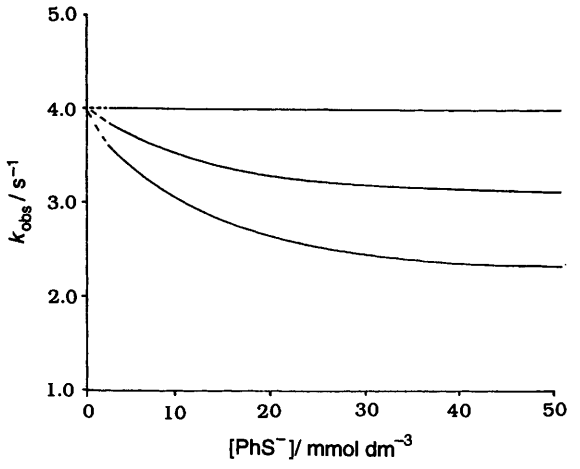

Fig. 4 Influence of the concentration of PhS^- on k_{obs} for the reaction of this thiolate with $[Cl_2FeS_2VS_2FeCl_2]^{3-}$ in MeCN at 25.0 °C, as predicted by the mechanism in Scheme 2 and equation (2). Curves drawn are those assuming: (bottom) both tetrahedral iron sites react independently, $2k_3 = k_2$; (top) the tetrahedral iron site in $[Cl_2FeS_2VS_2FeCl_2(SC_6H_4R\text{-}4)]^{4-}$ reacts twice as fast as either iron in $[Cl_2FeS_2VS_2FeCl_2]^{3-}$, $k_3 = k_2$ and (middle) the intermediate situation

caused by the $FeCl_2$ residues and the binding of a thiolate to one iron site results only in a minor additional change.

Attempts to detect the intermediate $[Cl_2FeS_2VS_2FeCl_2(SC_6H_4R\text{-}4)]^{4-}$ by Mössbauer or ^1H NMR spectra were unsuccessful. This species is too short-lived to be detectable over the protracted times necessary to accumulate a Mössbauer spectrum. In addition, significant concentrations of it are only produced in the presence of a large excess of thiolate. Under these conditions, ^1H NMR spectroscopy did not reveal any peaks clearly attributable to a short-lived intermediate, not even at −40 °C.

The mean values of K_1 for the binding of thiolate ion to $[Cl_2FeS_2VS_2FeCl_2]^{3-}$ (Table 1), cover the range 25–130 dm^3 mol^{-1}, depending on the thiolate. At a constant concentration of PhS^-, the addition of chloride ion, $[NEt_4Cl]$ = 0–30 mmol dm^{-3}, does not affect the value of K_1 and hence this rapid binding of thiolate does not result in chloride release. The rate of substitution of the cluster is not affected by the binding of the thiolate. This is consistent with rapid binding of $4\text{-}RC_6H_4S^-$ at one of the iron atoms to generate $[Cl_2FeS_2VS_2FeCl_2(SC_6H_4R\text{-}4)]^{4-}$, but it does not result in facile substitution. Consequently, $[Cl_2FeS_2VS_2FeCl_2(SC_6H_4R\text{-}4)]^{4-}$ undergoes substitution by a dissociative mechanism only at the tetrahedral iron site.

The rate law for the mechanism shown in Scheme 1 is given by equation (2) (see Appendix 1). It is derived assuming that: (*i*) $[Cl_2FeS_2VS_2FeCl_2]^{3-}$ is a steady-state intermediate; (*ii*) binding of the thiolate in the K_1 step is a rapid equilibrium reaction and (*iii*) dissociation of chloride from a tetrahedral iron is the rate-limiting step.

$$\frac{-d[Cl_2FeS_2VS_2FeCl_2{}^{3-}]}{dt} = \frac{(k_2 + k_3K_1[4\text{-}RC_6H_4S^-])[Cl_2FeS_2VS_2FeCl_2{}^{3-}]}{1 + K_1[4\text{-}RC_6H_4S^-]} \quad (2)$$

Since the two iron atoms in $[Cl_2FeS_2VS_2FeCl_2]^{3-}$ react as independent sites it is necessary to consider the relationship between k_2 and k_3. Although $[Cl_2FeS_2VS_2FeCl_2]^{3-}$ contains two reactive tetrahedral iron sites, in $[Cl_2FeS_2VS_2FeCl_2(SC_6H_4R\text{-}4)]^{4-}$ there is only one. If the two iron sites react entirely independently from one another the statistical relationship $k_2 = 2k_3$ is valid and equation (2) simplifies to (3).

$$\frac{-d[Cl_2FeS_2VS_2FeCl_2{}^{3-}]}{dt} = \frac{k_3(2 + K_1[4\text{-}RC_6H_4S^-])[Cl_2FeS_2VS_2FeCl_2{}^{3-}]}{1 + K_1[4\text{-}RC_6H_4S^-]} \quad (3)$$

The value of K_1 for each thiolate is known from the spectrophotometric analysis (Table 1). Using the data for the reaction with PhS^- (K_1 = 91.9 dm^3 mol^{-1}), and k_3 = 2 s^{-1}, we can simulate the dependence of k_{obs} on the concentration of thiolate ion, as defined by equation (3). This simulation is shown in Fig. 4 and has two important features. First, the values of k_{obs} decrease with increasing concentration of thiolate ion. Secondly, the effect of thiolate-ion concentration on the rate of reaction is small; the values of k_{obs} range from 2.3 to 3.6 (mean 3.0 ± 0.7 s^{-1}) which is in good agreement with the experimental data. The uncertainties associated with fitting the absorbance *vs.* time curves by two exponentials, and the errors inherent in calculating k_{obs}, means that it is not possible to discern such a small, regular variation. Careful inspection of our data reveals that satisfactory fits to the absorbance *vs.* time curves can be obtained in the range k_{obs} = 2.3–4.3 s^{-1} (mean 3.3 ± 1.0 s^{-1}).

However, an important feature of the $[Cl_2FeS_2VS_2FeCl_2(SPh)]^{4-}$ and $[Cl_2FeS_2VS_2FeCl_2]^{3-}$ clusters is that the overall charges differ, and the clusters are sufficiently small for this difference possibly to effect the lability of the iron sites. If the chloro-group on the tetrahedral iron in $[Cl_2FeS_2VS_2FeCl_2(SPh)]^{4-}$ dissociates slightly faster than a chloro-group in $[Cl_2FeS_2VS_2FeCl_2]^{3-}$ then the variation of k_{obs} with the concentration of thiolate would be even smaller than that simulated for $k_2 = 2k_3$. For instance, if $k_2 = 0.75k_3$, the effect would be as shown in Fig. 4 and the values of k_{obs} range from 3.8 ($[PhS^-]$ = 2) to 3.2 s^{-1} (50 mmol dm^{-3}), with a mean of 3.5 ± 0.3 s^{-1}. If the effect of the overall charge entirely annuls the statistical effect then, of course, $k_2 = k_3$, and equation (2) simplifies to $k_{obs} = k_2$. In presenting these simulations the effect has been illustrated using a large value of K_1, since this gives the largest variation in k_{obs}. Smaller values of K_1 result in even smaller effects than those illustrated in Fig. 4.

The mechanism shown in Scheme 2 rationalises why the rate of substitution of $[Cl_2FeS_2VS_2FeCl_2]^{3-}$ is independent of the concentration and nature of the thiolate, under conditions where binding of a thiolate to the cluster can clearly be detected.

In this study, for the first time, the binding of a thiolate to an iron–sulfur-based cluster has been detected spectroscopically. Certainly for other such clusters there is kinetic evidence that such binding occurs but this had not been supported spectroscopically.[2,8–11] In general, the binding of a nucleophile to these clusters does not significantly perturb their visible absorption spectra. However, the visible absorption spectra of $[Cl_2FeS_2VS_2FeCl_2]^{3-}$ and $[Cl_2FeS_2VS_2FeCl_2(SC_6H_4R\text{-}4)]^{4-}$ are sufficiently different for the binding of a thiolate to be evident.

A feature of the reactivity of $[Cl_2FeS_2VS_2FeCl_2]^{3-}$ is that binding of a thiolate to an iron atom 'switches off' the reactivity of this site. This reactivity pattern has been observed for other iron–sulfur-based clusters.[2,10] That binding of a nucleophile does not lead to substitution would, at first sight, appear strange, since once the nucleophile is bound apparently all that is required in order to form the product is dissociation of a chloro-group. However, the situation is more complicated, as illustrated by the qualitative reaction profiles for the associative and dissociative substitution pathways (Fig. 5). The profile for the dissociative pathway is illustrated on the left, and shows the two transition states corresponding to the formation of the three-co-ordinate intermediate, and the subsequent rapid attack by thiolate at this intermediate to form the product. On the right is the corresponding diagram for the associative pathway. Again, two transition states are evident, where the

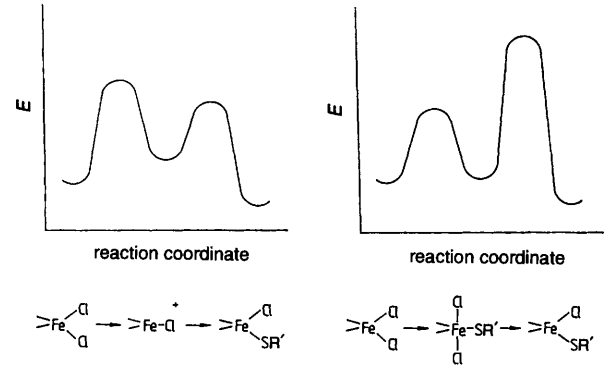

Fig. 5 Qualitative reaction profiles of the dissociative and associative pathways for the reaction of $[Cl_2FeS_2VS_2FeCl_2]^{3-}$ and $4\text{-}RC_6H_4S^-$; $R' = 4\text{-}RC_6H_4$

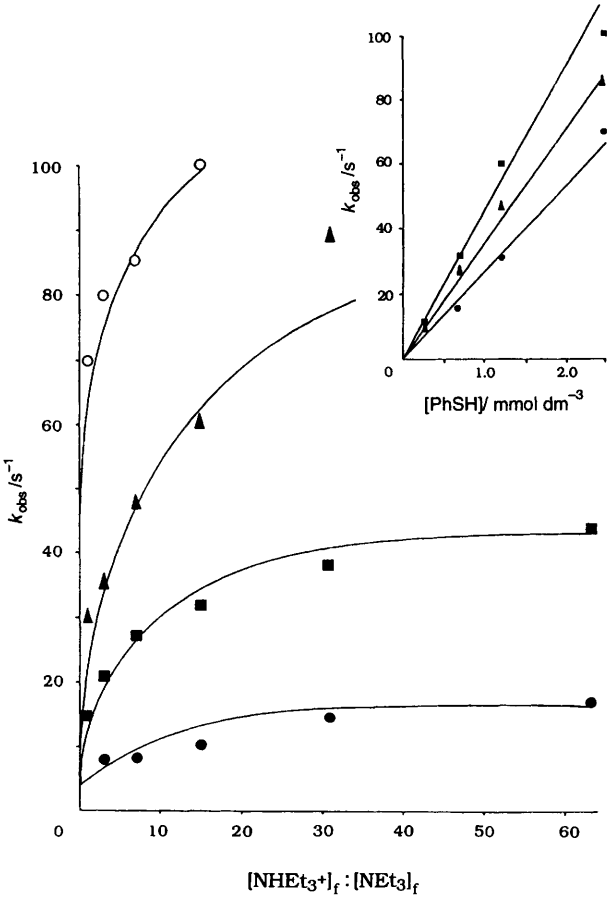

Fig. 6 Influence of $[NHEt_3^+]_f:[NEt_3]_f$ on k_{obs} for the reaction of $[Cl_2FeS_2VS_2FeCl_2]^{3-}$ (0.05 mmol dm^{-3}) with PhSH in MeCN at 25.0 °C. Data points correspond to [PhSH] = 0.31 (●), 0.63 (■), 1.25 (▲) and 2.5 mmol dm^{-3} (○). Curves drawn are those defined by Equation (7). Inset: influence of [PhSH] on k_{obs} for the reaction of $[Cl_2FeS_2VS_2FeCl_2]^{3-}$ (0.05 mmol dm^{-3}) in the presence of $[NHEt_3]^+$. Data points correspond to $[NHEt_3^+]_f:[NEt_3]_f$ = 1.0 (●), 7.0 (▲) and 15.0 (■)

first corresponds to the binding of the thiolate and the second to the dissociation of the chloro-group. Comparison of the relative energies of the transition states in these two profiles illustrates how the binding of thiolate to the iron in the associative route is more rapid than dissociation of a chloro-group in the dissociative pathway. However, the same diagrams also show that dissociation of a chloro-group in the associative pathway is slower than in the dissociative pathway. Consequently, although binding of the nucleophile can be a facile process it may not necessarily lead to a species which can rapidly form product.

The acid-catalysed reaction

The rate of substitution of $[Cl_2FeS_2VS_2FeCl_2]^{3-}$ by $[NEt_4][SPh]$ is accelerated in the presence of the weak acid $[NHEt_3][BPh_4]$. The absorbance *vs.* time traces can be fitted satisfactorily by two exponentials. Again, the discussion will focus on the initial substitution (*i.e.* the first exponential). Under all conditions ($[PhS^-] = 0.31$–2.5 mmol dm^{-3} and $[NHEt_3^+] = 0$–40.0 mmol dm^{-3}) the initial absorbance is that of $[Cl_2FeS_2VS_2FeCl_2]^{3-}$. That the traces are exponential indicates that the reaction is first order in the concentration of cluster. This is confirmed by studies in which the concentrations of acid, $[NHEt_3^+] = 10.0$ mmol dm^{-3} and thiolate, $[PhS^-] = 2.5$ mmol dm^{-3} are kept constant while the concentration of cluster is varied over the range 0.05–0.0031 mmol dm^{-3}. Under these conditions the value of the pseudo-first-order rate constant does not vary, $k_{obs} = 70.0 \pm 10\ s^{-1}$.

The studies on the uncatalysed reaction show spectroscopic evidence for binding of PhS^- to $[Cl_2FeS_2VS_2FeCl_2]^{3-}$. However, the relatively low concentrations of thiolate employed in the study of the acid-catalysed reaction mean that this binding is not detectable.

The dependences of the reaction rate on the concentrations of acid and thiolate were established by the method outlined in previous papers[2,8,9] involving systematic variation of the proportions of $[NHEt_3]^+$ and PhS^-. In order to calculate the concentrations of acid, base and nucleophile, the protolytic equilibrium (4) must be considered. Two limiting conditions are

$$[NHEt_3]^+ + PhS^- \rightleftharpoons NEt_3 + PhSH \qquad (4)$$

important. First, when $[NHEt_3^+] < [PhS^-]$ no free $[NHEt_3]^+$ is present and $k_{obs} = 3.3 \pm 1.0\ s^{-1}$, *i.e.* the substitution reaction occurs at the non-catalysed rate. It can be concluded that PhSH does not protonate $[Cl_2FeS_2VS_2FeCl_2]^{3-}$ in MeCN. Secondly, when $[NHEt_3^+] > [PhS^-]$ the concentrations of $[NHEt_3]^+$, NEt_3 and PhSH present in solution are given by equations (5) and (6) (subscript 'f' denotes the 'free' concentration). Under these conditions the reaction rate varies with both $[NHEt_3^+]_f$ and $[PhSH]_f$.

$$[NHEt_3^+]_f = [NHEt_3^+] - [PhS^-] \qquad (5)$$

$$[NEt_3]_f = [PhSH]_f = [PhS^-] \qquad (6)$$

The effect on k_{obs} of varying the ratio $[NHEt_3^+]_f:[NEt_3]_f$ is shown in Fig. 6. At a fixed concentration of PhSH the dependence of k_{obs} on this ratio is complicated. At low $[NHEt_3^+]_f:[NEt_3]_f$ the rate increases with the value of the ratio, while at high $[NHEt_3^+]_f:[NEt_3]_f$ it becomes independent of the ratio. The intercept on the k_{obs} axis corresponds to the uncatalysed reaction rate. In addition, increasing the concentration of PhSH affects the rate of the reaction. Under conditions where $[NHEt_3^+]_f:[NEt_3]_f$ is kept constant the reaction rate exhibits a linear dependence on [PhSH] (Fig. 6, inset).

The dependence on the ratio $[NHEt_3^+]_f:[NEt_3]_f$ can be analysed by the usual double-reciprocal graph,[12] from which the rate law (7) can be derived. The form of this rate law defines unambiguously the sequence of elementary reactions in the

$$\frac{-d[Cl_2FeS_2VS_2FeCl_2{}^{3-}]}{dt} = \frac{(1.59 \pm 0.35) \times 10^4\,[PhSH][NHEt^{3+}]_f/[NEt_3]_f[Cl_2FeS_2VS_2FeCl_2{}^{3-}]}{1 + 0.28 \pm 0.03([NHEt_3^+]_f/[NEt_3]_f)} \qquad (7)$$

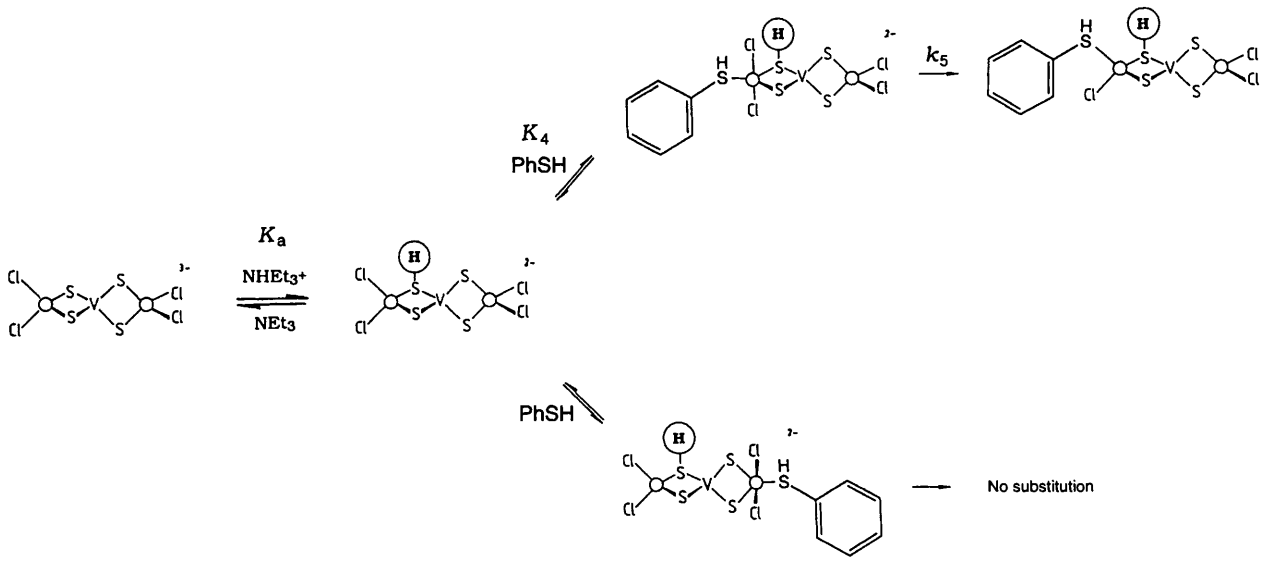

Scheme 3 Mechanism for the reaction between $[Cl_2FeS_2VS_2FeCl_2]^{3-}$ and PhSH in the presence of $[NHEt_3]^+$, at 25.0 °C in MeCN

acid-catalysed pathway. Thus, the numerator demonstrates that both a proton and PhSH must bind to the cluster before substitution can occur. Most importantly, the $[NHEt_3^+]_f/[NEt_3]_f$ term in the denominator shows that protonation of the cluster occurs before binding of the thiol. These features are shown in the mechanism in Scheme 3.

Previously, it has been shown[9] that $[NHEt_3]^+$ does not protonate the chloride ligands in iron–sulfur-based clusters, but rather protonation occurs at the cluster core. We propose that protonation of $[Cl_2FeS_2VS_2FeCl_2]^{3-}$ is at one of the μ-S atoms. However, this protonation is insufficiently labilising to result in dissociation of a chloro-group, and thiol must also bind to the cluster before substitution can occur.

Acid-catalysed, associative substitution mechanisms have been observed for other iron–sulfur-based clusters. However, this is the first study in which the stereochemical relationship between the sites of protonation and nucleophile binding can be defined. After the binding of the proton, PhSH can attack either the iron site adjacent to, or remote from, μ-SH (Scheme 3). Binding of a thiol and a proton at remote sites on this cluster results in a species where one iron is bound to the thiol and the other is adjacent to the bound proton, the μ-SH site. We have seen in the non-catalysed studies that the five-co-ordinate iron is not substitution labile in this complex. Similarly, the kinetics of the acid-catalysed reaction demonstrate that protonation alone is not labilising. We must conclude that acid-catalysed associative substitution is facile only when PhSH binds to the iron adjacent to the protonation site.

Protonation of the cluster at one of the bridging sulfur atoms 'switches off' the dissociative mechanism (observed in the non-catalysed pathway) and facilitates an associative mechanism. The electronic origin of this 'switching off' is readily understood. The addition of a proton to the cluster decreases the electron density on the adjacent iron site, thus strengthening the Fe–Cl σ bond and correspondingly decreasing the lability. Protonation can promote an associative mechanism by facilitating either attack of the nucleophile or dissociation of the leaving group. In the present system, by considering the kinetics, it is possible to distinguish between these two possibilities.

The rate law for the mechanism of Scheme 3 is shown in equation (8). It is readily derived by assuming that chloride dissociation is rate-limiting (k_5) and preceded by rapid protonation (K_a) and binding of thiol (K_4). Under the conditions employed in this study the reaction always exhibits a first-order dependence on the concentration of PhSH. Consequently, the term in the denominator $K_aK_4[PhSH][NHEt_3^+]_f/[NEt_3]_f$ can be neglected and equation (8) simplifies to (9) which is of the same form as that observed experimentally, equation (7). Comparison of equations (7) and (9) gives $K_a = 0.28 \pm 0.03$ and $k_5K_4 = (5.68 \pm 0.6) \times 10^4$ dm^3 mol^{-1} s^{-1}.

The associative pathway can be divided into two elementary reactions: binding of the thiol (K_4) and dissociation of the chloride leaving group (k_5). A limit to the values of K_4 and k_5 can be established in the following manner. Since the kinetics exhibits a simple first-order dependence on the concentration of PhSH, even at the highest concentration of thiol (2.5 mmol dm^{-3}), it is clear that $K_4[PhSH] \leqslant 0.2$. Consequently, $K_4 \leqslant 80$ dm^3 mol^{-1} and $k_5 \geqslant 7.1 \times 10^2$ s^{-1}. The important points concerning these values are as follows. (*i*) The dominant effect of protonating the cluster is to labilise the dissociation of the leaving chloro-group, $k_5/k_2 \geqslant 2.1 \times 10^2$. (*ii*) Protonation does not significantly increase the binding of the thiol to the cluster, $K_4/K_1 \leqslant 0.8$. (*iii*) The addition of only a proton or a thiolate is not significantly labilising; maximum labilisation of the chloro-group requires both the proton and the thiol to act synergically. Presumably, labilisation of the chloro-group in the acid-catalysed pathway is due to diminished π-electron density at the substituted iron site, caused by the electron-withdrawing influence of both the proton and the co-ordinated thiol.

Proton affinities of iron–sulfur-based clusters

The kinetics of the cluster substitution reactions was studied in acetonitrile, a solvent for which quantitative data concerning the nature of solution species are available.[13] The kinetic analysis for $[Cl_2FeS_2VS_2FeCl_2]^{3-}$ yields the value of K_a, which is the protolytic equilibrium constant defined by equation (10), where $K_a = K_a^{NHEt_3}/K_a^{cluster+H}$. Using the acid dissociation

$$\frac{-d[Cl_2FeS_2VS_2FeCl_2^{3-}]}{dt} = \frac{k_5K_4K_a[PhSH][Cl_2FeS_2VS_2FeCl_2^{3-}][NHEt_3^+]_f/[NEt_3]_f}{1 + (K_a[NHEt_3^+]_f/[NEt_3]_f) + (K_aK_4[PhSH][NHEt_3^+]_f/[NEt_3]_f)} \quad (8)$$

$$\frac{-d[Cl_2FeS_2VS_2FeCl_2^{3-}]}{dt} = \frac{k_5K_4K_a[PhSH][Cl_2FeS_2VS_2FeCl_2^{3-}][NHEt_3^+]_f/[NEt_3]_f}{1 + (K_a[NHEt_3^+]_f/[NEt_3]_f)} \quad (9)$$

Table 2 Mechanisms of substitution and acid strengths ($pK_a^{cluster+H}$) of protonated iron-sulfur-based clusters in MeCN at 25.0 °C

Cluster	Mechanism[a] Non-catalysed	Acid-catalysed	$pK_a^{cluster+H}$
1 $[VFe_2S_4Cl_4]^{3-}$	D	A	17.9[b]
2 $[S_2MoS_2FeCl_2]^{2-}$	A + D	A	17.9[14]
3 $[S_2WS_2FeCl_2]^{2-}$	A + D	A	18.1[14]
4 $[Fe_4S_4Cl_4]^{2-}$	A + D	A	18.8[9]
5 $[(MoFe_3S_4Cl_3)_2(\mu\text{-}SEt)_3]^{3-}$	A	A	18.6[9]
6 $[(MoFe_3S_4Cl_3)_2\{\mu\text{-}Fe(SEt)_6\}]^{3-}$	A	A	18.5[b]
7 $[Fe_4S_4(SR)_4]^{2-}$			
(R = Ph)	D	D	18.6[2]
(R = Et)	D	D	18.0[2]
8 $[\{MoFe_3S_4(SR)_3\}_2(\mu\text{-}SR)_3]^{3-}$			
(R = Ph)	D	A + D	17.9[8]
(R = Et)	—	A + D	18.1[8]
9 $[Fe_2S_2Cl_3(NCMe)]^-$	D	D	18.1[14]

[a] A = Associative, D = dissociative. [b] This work.

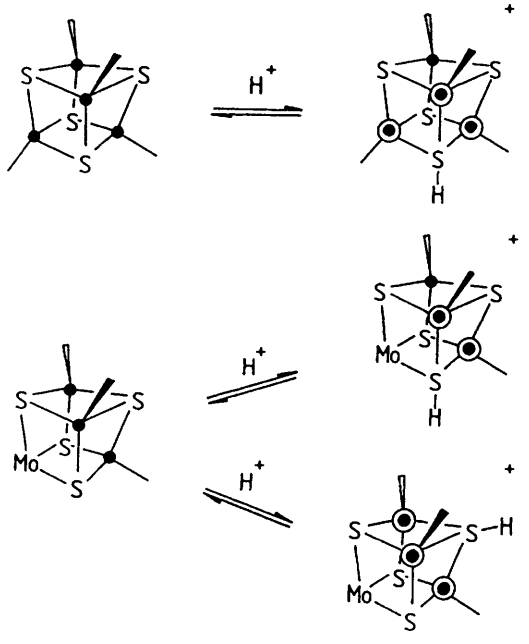

Scheme 4 Stereochemical relationship between sites of protonation and labilised iron sites (⊙) for acid-catalysed associative mechanisms at $\{Fe_4S_4\}^{2+}$ and $\{MoFe_3S_4\}^{3+}$ clusters

constant for $[NHEt_3]^+$ ($K_a^{NHEt_3}$ = 18.46 mol dm^{-3}), as defined by equation (11), the corresponding acid dissociation constant of the protonated cluster ($K_a^{cluster+H}$) can be calculated [equation (12)]. Inspection of Table 2 reveals that the values fall into the narrow range $17.9 < pK_a^{cluster+H} < 18.9$.

$$[cluster]^{n-} + [NHEt_3]^+ \overset{K_a}{\rightleftharpoons} [cluster + H]^{(n-1)} + NEt_3 \quad (10)$$

$$[NHEt_3]^+ \overset{K_a^{NHEt_3}}{\rightleftharpoons} NEt_3 + H^+ \quad (11)$$

$$[cluster + H]^{(n-1)-} \overset{K_a^{cluster+H}}{\rightleftharpoons} [cluster]^{n-} + H^+ \quad (12)$$

Previously[9] it has been pointed out that clusters such as $[Fe_4S_4Cl_4]^{2-}$, with ligands thermodynamically incapable of being protonated by $[NHEt_3]^+$, are associated with this range of $pK_a^{cluster+H}$. This demonstrates that protonation in these clusters must occur at the cluster core, presumably on a μ_3-S atom. Surprisingly, studies on clusters containing protonatable ligands, such as $[Fe_4S_4(SR)_4]^{2-}$ (R = alkyl or aryl), also have pK_a in the range 17.9–18.9.[2,8] This indicates that in these clusters also protonation is occurring on the μ_3-S atoms. It is important to emphasise that these pK_a values are determined from analyses of the kinetics of substitution reactions. It seems unlikely that the μ_3-S atoms are more basic than the thiolate ligands, however if protonation at a thiolate does occur, but does not effect the rate of substitution, then this protonation will go undetected by the kinetic method. It must be concluded that protonation of the cluster core (μ_3-S) is more labilising than protonation of the ligands in the substitution reactions of all iron–sulfur-based clusters.

It has been suggested that there is a significant difference in the basicity of μ-and μ_3-S atoms.[15] This is not consistent with the data shown in Table 2, where bi- and tri-nuclear clusters, which contain only μ-S atoms, have $pK_a^{cluster+H}$ values indistinguishable from those of cubane-type clusters, which contain only μ_3-S atoms.

Stereochemical aspects of acid-catalysed substitution mechanisms of iron–sulfur-based clusters

The studies on $[Cl_2FeS_2VS_2FeCl_2]^{3-}$ show that maximum labilisation is attained only when the proton binds to a sulfur adjacent to the nucleophile binding site. The question arises as to whether this stereochemical requirement is mandatory for other types of iron–sulfur-based clusters. In order to address this question as rigorously as possible, five features must be kept constant throughout all kinetic studies: leaving group (chloride ligand); nucleophile (PhSH); acid ($[NHEt_3]^+$); solvent (MeCN) and also substitution is restricted to tetrahedral iron sites. The top six entries in Table 2 are studies under which these conditions are fulfilled. The first three are linear clusters containing only μ-S atoms, and, in these clusters, the site of protonation *must* be adjacent to the site of substitution. Consistent with this, all three undergo acid-catalysed substitution by associative mechanisms.

Clusters **4**–**6** in Table 2 are cubane-based clusters and contain only μ_3-S atoms. Their higher nuclearity results in a more complicated situation. In the symmetrical, homonuclear $[Fe_4S_4Cl_4]^{2-}$ all iron sites are equivalent. However, upon protonation of a μ_3-S atom, the iron sites become differentiated: three iron atoms are adjacent to the μ_3-SH site whilst one is remote from it (Scheme 4).

On the basis of the available data it is not possible to distinguish which type of iron is substitutionally the more labile. However, $[Fe_4S_4Cl_4]^{2-}$ undergoes acid-catalysed substitution by an associative mechanism, and we have seen for $[Cl_2FeS_2VS_2FeCl_2]^{3-}$ that protonation facilitates an associative substitution mechanism at adjacent iron atoms. Conse-

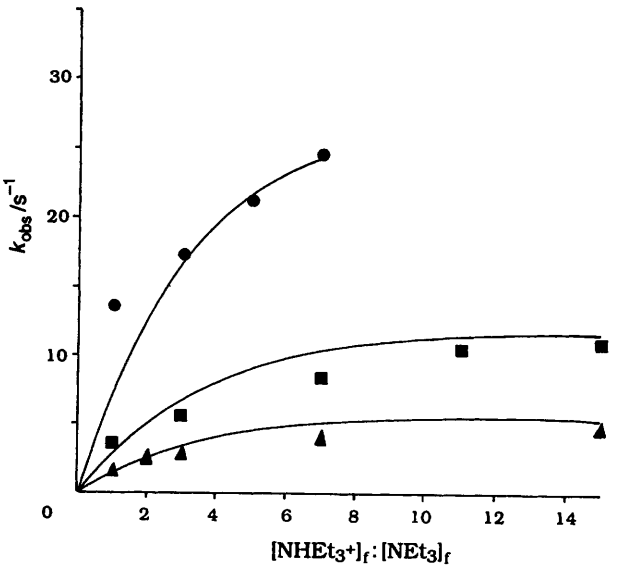

Fig. 7 Influence of $[NHEt_3^+]_f:[NEt_3]_f$ on k_{obs} for the reaction of $[(MoFe_3S_4Cl_3)_2\{\mu\text{-}Fe(SEt)_6\}]^{3-}$ (0.05 mmol dm^{-3}) with PhSH in MeCN at 25.0 °C. Data points correspond to [PhSH] = 5.0 (●), 2.5 (■) and, 1.25 mmol dm^{-3} (▲). Curves drawn are those defined by equation (A7)

quently, the reactivity of $[Fe_4S_4Cl_4]^{2-}$ is consistent with the three adjacent iron atoms being the sites of substitution.

A further degree of complexity arises for the $\{MoFe_3S_4\}^{3+}$-containing clusters. Prior to protonation, not all sulfur atoms in heteronuclear clusters are equivalent. Hence, protonation can occur at the three sulfurs bound to molybdenum or at the single, remote sulfur, as shown in Scheme 4. Protonation at the molybdenum-bound sulfur results in differentiation of the iron atoms (two are adjacent to the protonation site and one is remote), whilst protonation of the unique sulfur atom does not lead to differentiation of the irons. Again, the observation that both $[(MoFe_3S_4Cl_3)_2(\mu\text{-}SEt)_3]^{3-}$ (earlier work)[9] and $[(MoFe_3S_4Cl_3)_2\{\mu\text{-}Fe(SEt)_6\}]^{3-}$ (reported herein for the first time, Appendix 2) undergo acid-catalysed substitution reactions by associative mechanisms is consistent with the site of protonation being adjacent to the substitutionally most labile iron sites.

Structurally diverse iron–sulfur-based clusters all undergo acid-catalysed substitution reactions, and when the chloride ligand is the leaving group the mechanism is associative. It seems likely that in all these clusters protonation at μ-S atoms preferentially labilises adjacent iron sites to substitution.

Appendix 1

The rate law associated with the mechanism in Scheme 2 is most simply derived by considering the top and bottom of the Scheme independently. The rate law associated with the pathway on the top is shown in equation (A1), where the

$$\frac{-d[Cl_2FeS_2VS_2FeCl_2^{3-}]}{dt} = \frac{k_2k_4[4\text{-}RC_6H_4S^-][Cl_2FeS_2VS_2FeCl_2^{3-}]_f}{k_{-2}[Cl^-] + k_4[4\text{-}RC_6H_4S^-]} \quad (A1)$$

subscript f denotes an equilibrium concentration. This equation is derived assuming that $[Cl_2FeS_2VS_2FeCl]^{2-}$ is a steady-state intermediate, which can either rebind the chloride ion (k_{-2}), to regenerate the starting material, or be attacked by thiolate ion (k_4) to accomplish the substitution reaction.

When the kinetics is studied in the presence of chloride ion, $[NEt_4Cl]$ = 0–30 mmol dm^{-3}, under conditions where the concentration of thiolate ion is kept constant, $[PhS^-]$ = 10 mmol dm^{-3}, the value of k_{obs} does not vary, 5.0 s^{-1}, and the rate of the reaction remains insensitive to the concentration of thiolate ion. Hence, $k_4/k_{-2} \geqslant 3$, and $k_{-2}[Cl^-] \ll k_4[4\text{-}RC_6H_4S^-]$ under all experimental conditions used in this study, and equation (A1) simplifies to (A2).

$$-d[Cl_2FeS_2VS_2FeCl_2^{3-}]/dt = k_2[Cl_2FeS_2VS_2FeCl_2^{3-}]_e \quad (A2)$$

In an analogous manner the rate law for the pathway on the bottom of Scheme 2 is derived, as shown in equation (A3). Combining equations (A2) and (A3), the *total* rate for the substitution reaction can be described by (A4).

$$-d[Cl_2FeS_2VS_2FeCl_2^{3-}]/dt = k_3[Cl_2FeS_2VS_2FeCl_2(SC_6H_4R)^{4-}]_f \quad (A3)$$

$$-d[Cl_2FeS_2VS_2FeCl_2^{3-}]/dt = k_2[Cl_2FeS_2VS_2FeCl_2^{3-}]_f + k_3[Cl_2FeS_2VS_2FeCl_2(SC_6H_4R)^{4-}]_f \quad (A4)$$

The relationship between $[Cl_2FeS_2VS_2FeCl_2^{3-}]_f$, $[Cl_2FeS_2VS_2FeCl_2(SC_6H_4R)^{4-}]_f$ and the total concentration of cluster, $[Cl_2FeS_2VS_2FeCl_2^{3-}]_T$, is readily derived and is shown in equation (A5). Using equations (A4) and (A5) to express all terms with respect to $[Cl_2FeS_2VS_2FeCl_2^{3-}]_T$, the full rate law for the substitution reactions of $[Cl_2FeS_2VS_2FeCl_2]^{3-}$ is obtained [equation (A6)].

$$[Cl_2FeS_2VS_2FeCl_2^{3-}]_T = (1 + K_1[4\text{-}RC_6H_4S^-])[Cl_2FeS_2VS_2FeCl_2^{3-}]_e \quad (A5)$$

$$\frac{-d[Cl_2FeS_2VS_2FeCl_2^{3-}]}{dt} = \frac{(k_2 + k_3K_1[4\text{-}RC_6H_4S^-])[Cl_2FeS_2VS_2FeCl_2^{3-}]_T}{1 + K_1[4\text{-}RC_6H_4S^-]} \quad (A6)$$

Appendix 2

The kinetic data for both the non-catalysed and the acid-catalysed reactions of $[(MoFe_3S_4Cl_3)_2\{\mu\text{-}Fe(SEt)_6\}]^{3-}$ are illustrated in Fig. 7.

In the absence of acid, the substitution of the first chloro-group exhibits a simple first-order dependence on the concentrations of both cluster and PhS^-, consistent with the associative mechanism shown in Scheme 5. The derived value of $K_2k_3 = 5.2 \times 10^3$ dm^3 mol^{-1} s^{-1} for $[(MoFe_3S_4Cl_3)_2\{\mu\text{-}Fe(SEt)_6\}]^{3-}$ is about three times slower than the corresponding value for $[(MoFe_3S_4Cl_3)_2(\mu\text{-}SEt)_3]^{3-}$ ($K_2k_3 = 1.7 \times 10^4$ dm^3 mol^{-1} s^{-1}).

In the presence of acid, the rate of reaction exhibits the usual non-linear dependence on the ratio $[NHEt_3^+]:[NEt_3]$, as shown in Fig. 7. In addition, the rate of the reaction exhibits a first-order dependence on the concentration of PhSH. This behaviour is consistent with the acid-catalysed associative mechanism shown in Scheme 5. The rate law associated with this mechanism is shown in equation (A7). Analysis of the data gives the values $k_3^HK_2^H = 8.26 \times 10^3$ dm^3 mol^{-1} s^{-1} and K_a = 0.23 dm^3 mol^{-1} for $[(MoFe_3S_4Cl_3)_2\{\mu\text{-}Fe(SEt)_6\}]^{3-}$. These values are similar to those observed for $[(MoFe_3S_4Cl_3)_2(\mu\text{-}SEt)_3]^{3-}$ ($k_3^HK_2^H = 4.0 \times 10^3$ dm^3 mol^{-1} s^{-1} and K_a = 1.2 dm^3 mol^{-1}.[9]

$$\frac{-d[(MoFe_3S_4Cl_3)_2\{\mu\text{-}Fe(SEt)_6\}^{3-}]}{dt} = \frac{k_3^HK_2^HK_a[(MoFe_3S_4Cl_3)_2\{\mu\text{-}Fe(SEt)_6\}^{3-}][PhSH][NHEt_3^+]_f/[NEt_3]_f}{1 + (K_a[NHEt_3^+]_f/[NEt_3]_f)} \quad (A7)$$

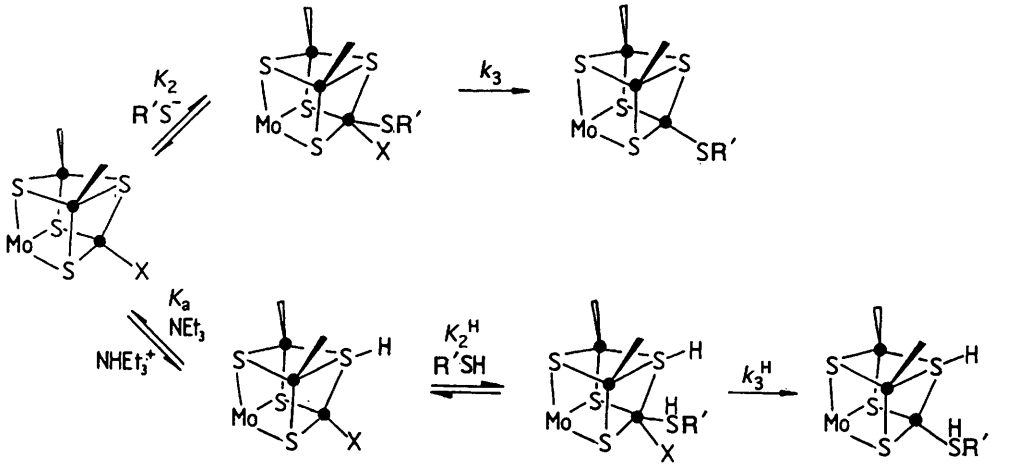

Scheme 5 Mechanism for the reaction between $[(MoFe_3S_4Cl_3)_2\{\mu\text{-}Fe(SEt)_6\}]^{3-}$ and PhSH in the presence of $[NHEt_3]^+$, at 25.0 °C in MeCN

It is interesting to note the differences in the elementary rate constants for the reactions of $[(MoFe_3S_4Cl_3)_2\{\mu\text{-}Fe(SEt)_6\}]^{3-}$ and $[(MoFe_3S_4Cl_3)_2(\mu\text{-}SEt)_3]^{3-}$. Both contain the same subcluster, $\{MoFe_3S_4Cl_3\}$, the only distinction being the nature of the ligands bound to molybdenum. That $[(MoFe_3S_4Cl_3)_2\{\mu\text{-}Fe(SEt)_6\}]^{3-}$ is less labile than $[(MoFe_3S_4Cl_3)_2(\mu\text{-}SEt)_3]^{3-}$ in the uncatalysed substitution reaction is consistent with the μ-$Fe(SEt)_6$ group being more electron withdrawing than the μ-$(SEt)_3$ moiety. In the acid-catalysed reactions the greater electron-withdrawing effect of μ-$Fe(SEt)_6$ results in a smaller value of K_a, but a greater lability of the protonated cluster as measured by the value of $k_3^H K_2^H$.

Acknowledgements

We thank Dr. D. J. Evans and Mrs. J. E. Barclay for help and advice on Mössbauer techniques and interpretation of Mössbauer results, and, the John Innes Foundation for a studentship (to K. L. C. G.).

References

1 R. Cammack, *Adv. Inorg. Chem.*, 1992, **38**, 281 and refs. therein.
2 R. A. Henderson and K. E. Oglieve, *J. Chem. Soc., Dalton Trans.*, 1993, 1467.
3 V. Do, E. D. Simhon and R. H. Holm, *Inorg. Chem.*, 1985, **24**, 4635.
4 R. E. Palermo, P. P. Power and R. H. Holm, *Inorg. Chem.*, 1982, **21**, 173.
5 J. R. Dilworth, R. A. Henderson, P. Dahlstrom, T. Nicholson and J. A. Zubieta, *J. Chem. Soc., Dalton Trans.*, 1987, 529.
6 R. A. Henderson, *J. Chem. Soc., Dalton Trans.*, 1982, 917.
7 R. H. Holm, *Adv. Inorg. Chem.*, 1992, **38**, 1 and refs. therein.
8 R. A. Henderson and K. E. Oglieve, *J. Chem. Soc., Dalton Trans.*, 1993, 1473.
9 R. A. Henderson and K. E. Oglieve, *J. Chem. Soc., Chem. Commun.*, 1994, 377.
10 R. A. Henderson and K. E. Oglieve, *J. Chem. Soc., Chem. Commun.*, 1994, 1961.
11 R. A. Henderson, *J. Chem. Soc., Chem. Common.*, 1995, 1905.
12 R. G. Wilkins, *Kinetics and Mechanism of Reactions of Transition Metal Complexes*, VCH, Weinheim, 1991, p. 24.
13 J. F. Coetzee, *Prog. Phys. Org. Chem.*, 1967, **4**, 45.
14 K. L. C. Grönberg, R. A. Henderson and K. E. Oglieve, unpublished work.
15 I. G. Dance, *Aust. J. Chem.*, 1994, **47**, 979.

Received 28*th May* 1996; *Paper* 6/03658I